N87-18033 UNCLAS

MICROCOPY RESOLUTION TEST CHART
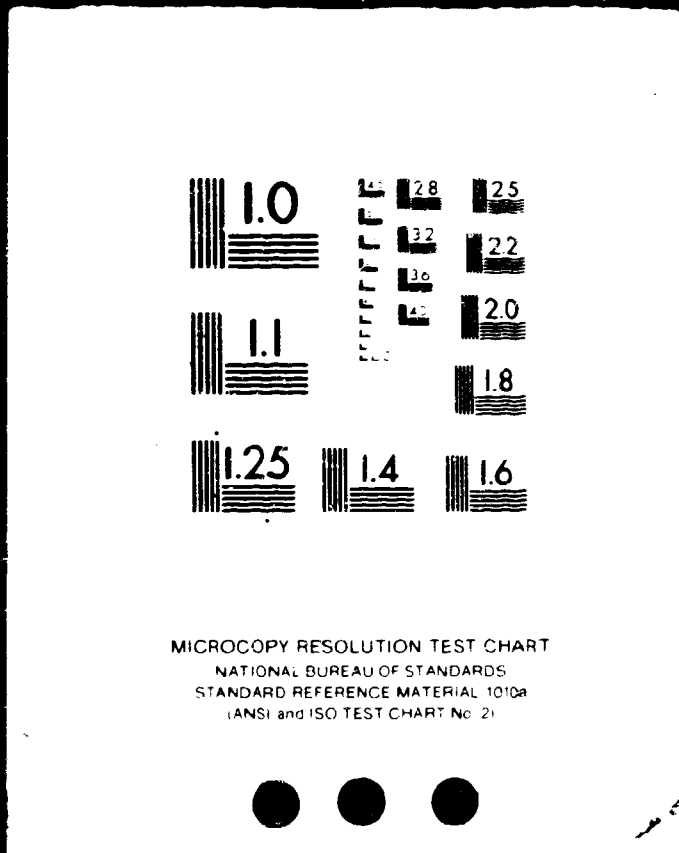NATIONAL BUREAU OF STANDARDS
STANDARD REFERENCE MATERIAL 1010a
(ANSI and ISO TEST CHART No. 2)

NASA Contractor Report 178233

ICASE REPORT NO. 87-4

ICASE

FINITE ELEMENT FLUX-CORRECTED TRANSPORT (FEM-FCT)

FOR THE EULER AND NAVIER-STOKES EQUATIONS

Rainald Lohner

Ken Morgan

Jaime Peraire

Mehdi Vahdati

NASA
National Aeronautics and
Space Administration

Langley Research Center
Hampton, Virginia 23665

FINITE ELEMENT FLUX-CORRECTED TRANSPORT (FEM-FCT)

FOR THE EULER AND NAVIER-STOKES EQUATIONS

Rainald Löhner

Berkeley Research Associates
Springfield, VA 22150, USA
and
Laboratory for Computational Physics and Fluid Dynamics
Naval Research Laboratory
Washington, D.C. 20375, USA

Ken Morgan, Jaime Peraire and Mehdi Vahdati

Institute for Numerical Methods in Engineering
University of Wales
Swansea SA2 8PP, Wales, U.K.

ABSTRACT

A high resolution finite element method for the solution of problems involving high speed compressible flows is presented. The method uses the concepts of flux-corrected transport and is presented in a form which is suitable for implementation on completely unstructured triangular or tetrahedral meshes. Transient and steady state examples are solved to illustrate the performance of the algorithm.

INTRODUCTION

Over the past few years. there has been an ongoing interest in the application of unstructured grid finite element methods to the solution of problems of high speed compressible flow. In this area. the authors [18-20] have proposed a two-step explicit implementation of a second order Taylor-Galerkin procedure [16.17] and have used this approach to solve successfully a variety of inviscid and viscous problems. The addition of artificial viscosity is required to stabilize this solution procedure when it is applied to the analysis of problems involving strong discontinuities. and this has the effect of spreading flow discontinuities over several computational cells.

Solution methods based upon high resolution schemes [1-6] give sharper definition of flow discontinuities and are supposedly more robust. In two and three dimensions. these methods are generally implemented by using operator splitting and applying

Here ρ, p, ϵ, T and k denote the density, pressure, specific total energy, temperature and thermal conductivity of the fluid respectively and u_i is the component of the fluid velocity in the direction x_i of a Cartesian coordinate system. The equation set is completed by the addition of the state equations

$$p = (\gamma - 1)\rho[\epsilon - \frac{1}{2}u_j u_j] \quad , \quad T = c_v[\epsilon - \frac{1}{2}u_j u_j] \quad . \tag{3}$$

which are valid for a perfect gas, where γ is the ratio of the specific heats and c_v is the specific heat at constant volume. The components of the viscous stress tensor σ_{ij} are given by

$$\sigma_{ij} = \mu(\frac{\partial u_i}{\partial x_j} + \frac{\partial u_j}{\partial x_i}) + \lambda \frac{\partial u_k}{\partial x_k}\delta_{ij} \tag{4}$$

and it is assumed that λ and μ are related by

$$\lambda = -\frac{2\mu}{3} \tag{5}$$

THE FLOW SOLVER: FEM-FCT

As stated above, high resolution, monotonicity preserving schemes must be developed in order to be able to simulate the strong nonlinear discontinuities present in the flows under consideration. Although the pertinent literature abounds with high resolution schemes [1-6], only Zalesak's generalization [7] of the 1-D FCT schemes of Boris and Book [8-10] can be considered a truly multidimensional high resolution scheme. We remark here that the use of unstructured grids requires such truly multidimensional schemes, as the lack of lines or planes in the mesh inhibits the use of operator splitting.

Erlebacher [11], and Parrot and Christie [12] first analyzed FCT schemes in the context of finite element methods. We develop their ideas further to include the consistent mass, which yields high temporal accuracy, and to systems of equations.

The Concept of Flux-Corrected Transport (FCT)

We consider a set of conservation laws given by a system of partial differential equations of the form given in eqn.(1), and assume that the advective fluxes $F^a = F^a(U)$ play a dominant role over the viscous fluxes $F^v = F^v(U)$. For flows described by eqn.(1), discontinuities in the variables may arise (e.g. shocks or contact discontinuities). Any numerical scheme of order higher than one will produce overshoots or ripples at such discontinuities (the so-called 'Godunov theorem' [15]). Very often, particularly for mildly nonlinear systems, these overshoots can be tolerated. However, for the class of problems studied here, overshoots will eventually lead to numerical instability, and will therefore have to be suppressed.

2

The idea behind FCT is to combine a high-order scheme with a low-order scheme in such a way that in regions where the variables under consideration vary smoothly (so that a Taylor expansion makes sense) the high-order scheme is employed, whereas in those regions where the variables vary abruptly the schemes are combined, in a conservative manner, in an attempt to ensure a monotonic solution.

The temporal discretization of eqn.(1) yields

$$U^{n+1} = U^n + \Delta U. \tag{6}$$

where ΔU is the increment of the unknowns obtained for a given scheme at time $t = t^n$. Our aim is to obtain a ΔU of as high an order as possible without introducing overshoots. To this end, we re-write eqn.(6) as:

$$U^{n+1} = U^n + \Delta U^l + (\Delta U^h - \Delta U^l). \tag{7}$$

or

$$U^{n+1} = U^l + (\Delta U^h - \Delta U^l). \tag{8}$$

Here ΔU^h and ΔU^l denote the increments obtained by some high- and low-order scheme respectively, whereas U^l is the monotone, ripple-free solution at time $t = t^{n+1}$ of the low-order scheme. The idea behind FCT is to limit the second term on the right-hand side of eqn.(8):

$$U^{n+1} = U^l + lim(\Delta U^h - \Delta U^l). \tag{9}$$

in such a way that no new over/undershoots are created.

It is at this point that a further constraint, given by the conservation law (1) itself must be taken into account: strict conservation on the discrete level should be maintained. The simplest way to guarantee this for node-centered schemes (and we will only consider those here) is by constructing schemes for which the sum of the contributions of each individual element (cell) to its surrounding nodes vanishes ('all that comes in goes out'). This means that the limiting process (eqn.(9)) will have to be carried out in the elements (cells).

Algorithmic Implementation

We can now define FCT in a quantitative way. We follow Zalesak's exposition [7]. but modify the term 'flux' by 'element contribution to a node'. Those more familiar with finite volume or finite difference schemes should replace 'element' by 'cell' in what follows.

FCT consists of the following six algorithmic steps:

1) Compute LEC: the 'low-order element contribution' from some low-order scheme guaranteed to give monotonic results for the problem at hand;

2) Compute HEC: the 'high-order element contribution', given by some high-order scheme;

3) Define AEC: the 'antidiffusive element contributions':

$$AEC = HEC - LEC$$

4) Compute the updated low-order solution:

$$U^l = U^n + \sum_{el} LEC = U^n + \Delta U^l \tag{10}$$

5) Limit or 'correct' the AEC so that U^{n+1} as computed in step 6 below is free of extrema not also found in U^l or U^n:

$$AEC^c = Cel * AEC, \quad 0 \le Cel \le 1; \tag{11}$$

6) Apply the limited AEC:

$$U^{n+1} = U^l + \sum_{el} AEC^c. \tag{12}$$

The Limiting Procedure

Obviously, the whole approach depends critically on the all-important step 5 above. We define the following quantities:

a) $P_I^\pm$: the sum of all positive (negative) antidiffusive element contributions to node I

$$P_I^\pm = \sum_{el} \begin{Bmatrix} max \\ min \end{Bmatrix} (0, AEC_{el})$$

b) $Q_I^\pm$: the maximum (minimum) increment (decrement) node I is allowed to achieve in step 6 above

$$Q_I^\pm = U_I^{\,max\,min} - U^l$$

where $U_I^{\,max\,min}$ (defined below) represents the maximum (minimum) value the unknown U at node I is allowed to achieve in step 6 above.

c) $R^\pm$:

$$R^\pm := \begin{cases} min(1, Q^\pm/P^\pm) & if \;\; P^+ > 0, \; P^- < 0 \\ 0 & if \;\; P^\pm = 0 \end{cases} .$$

Now take, for each element:

$$Cel = min(element\ nodes) \begin{cases} R^+ & if\ AEC > 0. \\ R^- & if\ AEC < 0. \end{cases} \qquad (13)$$

Finally, we obtain $U_I^{max}_{min}$ in three steps :

a) maximum (minimum) nodal U of U^n and U^l :

$$U_I^* = \begin{Bmatrix} max \\ min \end{Bmatrix} (U_I^l, U_I^n)\ .$$

b) maximum (minimum) nodal value of element :

$$U_{el}^* = \begin{Bmatrix} max \\ min \end{Bmatrix} (U_A^*, U_B^*, ..., U_C^*)\ .$$

where $A, B, ..., C$ represent the nodes of element el.

c) maximum (minimum) U of all elements surrounding node I :

$$U_I^{max}_{min} = \begin{Bmatrix} max \\ min \end{Bmatrix} (U_1^*, U_2^*, ..., U_m^*)\ .$$

where $1, 2, ..., m$ represent the elements surrounding node I.

This completes the description of the limiting procedure. Up to this point we have been completely general in our description, so that eqns.(6)-(13) may be applied to any FEM-FCT scheme. In what follows, we restrict the exposition to the finite element schemes employed in the present work, describing the high and low-order schemes used.

The High-Order Scheme: Consistent-Mass Taylor Galerkin

As the high-order scheme, we employ a two-step form [18-20] of the one-step Taylor-Galerkin schemes described in [16,17]. These schemes belong to the Lax-Wendroff class, and could be substituted by any other high-order scheme which appears more convenient, including implicit schemes. Given the system of equations (1), we advance the solution from t^n to $t^{n+1} = t^n + \Delta t$ as follows:

a) First step (advective predictor):

$$U^{n+\frac{1}{2}} = U^n - \frac{\Delta t}{2} \cdot \frac{\partial F_j^a}{\partial x_j}\Big|^n \qquad (14)$$

b) Second step :

$$\Delta U^n = U^{n+1} - U^n = -\Delta t \frac{\partial F_j^a}{\partial x_j}\Big|^{n+\frac{1}{2}} + \Delta t \frac{\partial F_j^v}{\partial x_j}\Big|^n \qquad (15)$$

5

The spatial discretization of (14) and (15) is performed via the classic Galerkin weighted residual method [18-20], using linear elements, i.e. 3-noded triangles in 2-D and 4-noded tetrahedra in 3-D. For (15) the following system of equations is obtained:

$$M_C \cdot \Delta U^n = R^n. \tag{16}$$

where M_C denotes the consistent mass matrix [18-20], ΔU the vector of nodal increments and R the vector of added element contributions to the nodes. As M_C possesses an excellent condition number, eqn.(16) is never solved directly, but iteratively, requiring typically three passes [17]. We recast the converged solution of eqn.(16) into the following form, which will be of use later on :

$$M_L \cdot \Delta U^h = R + (M_L - M_C) \cdot \Delta U^h. \tag{17}$$

Here M_L denotes the diagonal, lumped mass-matrix (see [17]).

The Low-Order Scheme: Lumped-Mass Taylor Galerkin plus Diffusion

The requirement placed on the low-order scheme in any FCT-method is monotonicity. The low-order scheme must not produce any artificial, or numerical, 'ripples' or 'wiggles'. It is clear that the better the low-order scheme, the easier the resulting task of limiting will be. Therefore an obvious candidate for the low-order scheme is Godunov's method [15]. However, this scheme would be relatively expensive, and its extension to unstructured grids remains unclear.

We have so far added 'mass-diffusion' to the lumped-mass Taylor-Galerkin scheme in the context of FEM-FCT [13,14]. This simplest and least expensive form of diffusion is obtained by subtracting the lumped mass-matrix from the consistent mass-matrix for linear elements:

$$DIFF = c_d \cdot (M_C - M_L) \cdot U^n. \tag{18}$$

The element matrix thus obtained for 2-D triangles is of the form

$$c_d \cdot (M_C - M_L)_{el} = - \frac{c_d \cdot Vol_{el}}{12} \left\{ \begin{array}{ccc} 2 & -1 & -1 \\ -1 & 2 & -1 \\ -1 & -1 & 2 \end{array} \right\} \tag{19}$$

Observe that we cannot simply add this diffusion to the high-order scheme in order to obtain monotonic results, as a multipoint-coupling of the right-hand side occurs due to the consistent mass-matrix employed in the high-order scheme . The imposition of monotonicity can nevertheless be achieved by using a lumped mass-matrix instead. As the terms originating from the discretization of the fluxes F^i in (1) are the same as in (15), the low-order scheme is given by

$$M_L \cdot \Delta U^l = R + DIFF. \tag{20}$$

6

Resulting Antidiffusive Element Contributions

Subtracting (20) from (17) yields the equation

$$M_L \cdot (\Delta U^h - \Delta U^l) = R + (M_L - M_C) \cdot \Delta U^h - R - DIFF, \tag{21}$$

or. using eqn.(18)

$$\Delta U^h - \Delta U^l = M_l^{-1} \cdot (M_L - M_C) \cdot (c_d \cdot U^n + \Delta U^h). \tag{22}$$

Note that all terms arising from the discretization of the fluxes F^i in (1),(15),(20) have now disappeared. This is of particular importance if the antidiffusive element contributions must be recomputed (small core memory machines), and real gas effects

are taken into account (table look-up times are considerable) or real viscosity effects have to be included (Navier-Stokes equations).

Limiting for Systems of Equations

The results available in the literature [8-10] and our own experience [13,14] have shown that with FCT results of excellent quality can be obtained for a single PDE. However, when trying to extend the limiting process to systems of PDEs. no immediately obvious or natural limiting procedure becomes apparent. Obviously, for 1-D problems one could advect each simple wave system separately, and then assemble the solution at the new time step. However. for multidimensional problems such a splitting is not possible, as the acoustic waves are circular. FDM-FCT-codes used for production runs [21,22] have so far limited each equation separately, invoking operator-splitting arguments. This approach does not always give very good results, as may be seen from Sod's comparison of schemes for the Riemann problem [23]. and has been a point of continuing criticism by those who prefer to use the more costly Riemann-solver-based, essentially one-dimensional TVD-schemes [1-6]. It would therefore appear as attractive to introduce 'system character' for the limiter by combining the limiters for all

some undershoots for very strong shocks are present. This option is currently our preferred choice for transient problems.

iii) Use of the minimum of the limiters obtained for the density and the pressure ($C_{el} = min(C_{el}(density), C_{el}(pressure))$) : this again produces acceptable results, particularly for steady-state problems.

NUMERICAL EXAMPLES

a) Shock over an indentation: The first problem considered simulates the transient flowfield produced by the interaction of a strong shock with an indentation in the ground. For this case, the shock Mach number was set to $M_s = 25$, which corresponds to a pressure-jump ratio of about 1:100. During the transient, pressure ratios as high as 1:1000 result. The problem statement, solution domain, spatial discretization and solutions obtained are shown in Figs.1a-1e. Note that an adaptive refinement scheme for transient problems [26] was used to reduce the overall storage and CPU requirements.

As the shock travels over the indentation, it produces a bow shock and a rarefaction (Figs.1a,1b). Then, it collides with the right wall of the indentation and bounces back, producing several shock/shock and shock/contact discontinuity interactions (Figs.1c,1d). Observe the level of physically relevant detail that the scheme is able to reproduce, e.g. the triple shock produced at T=0.12 (Figs.1d,1e). The velocity pattern generated by these interactions has been magnified in Fig.1e, and shows a large residual vortex, as well as the different shock fronts and other discontinuities. We remark that at all times the shocks are captured within 2 to 3 elements.

In the present case, we used as limiter for all equations the minimum of the limiters computed for the continuity and energy equations. It is found, that for the strong shocks present in such flowfields, even a pressure-undershoot of 0.1% will lead to negative pressures. Therefore, the pressure is additionally limited artificially in order to be positive (albeit small) at all times.

b) Steady supersonic flow past a circular cylinder: This problem involves inviscid Mach 3 flow past a circular cylinder. The solution has been obtained by relaxing, with local timesteps, the transient solution towards the final steady-state. During this iteration process, the grid was adapted three times to the solution by using an adaptive mesh regeneration technique [27]. The final grid is shown in Fig.2a. A detail of the pressure coefficient distribution is shown in Fig.2b, and the variation of pressure coefficient along the centre line and over the cylinder surface is given in Fig.2c.

c) Shock-bubble interaction: This problem is included here to demonstrate a new axisymmetric capability, and also to show that not only geometrically complex domains, but also physically complex problems can be handled economically by the methodologies developed. Initially, a weak shock ($M_s = 1.29$), coming from the left in Fig.3a, travels into a bubble of heavier material. In the present case, the outer medium was assumed to be air, while the bubble was assumed to consist of freon. Due to the higher density of freon, the shock speed inside the bubble decreases (Fig.3b). While the outer

shock bends over. the inner shock focuses at the right end of the bubble. producing a significant overpressure (Fig.3c). and initiating a small. circular blast wave (Fig.3d).

__d) Steady supersonic flow over a flat plate:__ The fourth problem considered is the steady state solution of supersonic viscous flow over a flat plate. The flow conditions correspond identically to one of the cases considered by Carter [28]. using a finite difference scheme. The free stream Mach number is 3 and the Reynolds number based on the plate length is 1000. The temperature of the plate is assumed constant. The Sutherland viscosity law (see. e.g. Schlichting [29]) is used and the initial conditions are chosen to be appropriate to the case of a flat plate impulsively inserted into the free stream. The mesh used is displayed in Fig.4a. and the general features of the solution can be appreciated in the density contour plots shown in Fig.4b. The variation of the computed wall pressure distribution is given in Fig.4c.

CONCLUSIONS

It has been demonstrated how unstructured grids and high resolution schemes may be combined. yielding FEM-FCT. The numerical examples indicate that a high accuracy can be obtained economically for problems involving complex domains and/or adaptive mesh refinement. Furthermore, the 'equation-splitting' employed in classic FCT-codes [21.22] has been extended by coupling or 'synchronizing' the limiters of all the equations involved, without taking recourse to more costly Riemann-solver-based monotone schemes.

Extensions of the present work are under investigation and involve the development of better limiters for systems of equations in the context of FEM-FCT, the extension of FEM-FCT to implicit or semi-implicit time-stepping schemes [31], and the combination of FEM-FCT with unstructured multigrid methods [32] for the rapid solution of steady state problems.

ACKNOWLEDGEMENTS

REFERENCES

[1] P. Woodward and P. Colella - The Numerical Simulation of Two-Dimensional Fluid Flow with Strong Shocks; *J.Comp.Phys.* 54, 115-173 (1984).

[2] B. van Leer - Towards the Ultimate Conservative Scheme. II. Monotonicity and Conservation Combined in a Second order Scheme; *J.Comp.Phys.* 14. 361-370 (1974).

[3] P.L. Roe - Approximate Riemann Solvers. Parameter Vectors and Difference Schemes; *J.Comp.Phys.* 43, 357-372 (1981).

[4] S. Osher and F. Solomon - Upwind Difference Schemes for Hyperbolic Systems of Conservation Laws; *Math.Comp.* 38, 339-374 (1982).

[5] A. Harten - High Resolution Schemes for Hyperbolic Conservation Laws: *J.Comp.Phys.* 49, 357-393 (1983).

[6] P.K. Sweby - High Resolution Schemes Using Flux Limiters for Hyperbolic Conservation Laws; *SIAM J.Num.Anal.* 21, 995-1011 (1984).

[7] S.T. Zalesak - Fully Multidimensional Flux-Corrected Transport Algorithm for Fluids; *J.Comp.Phys.* 31, 335-362 (1979).

[8] J.P. Boris and D.L. Book - Flux-corrected Transport. I. SHASTA, a Transport Algorithm that works; *J.Comp.Phys.* 11, 38 (1973).

[9] D.L. Book, J.P. Boris and K. Hain - Flux-corrected Transport. II. Generalizations of the Method; *J.Comp.Phys.* 18, 248 (1975).

[10] J.P. Boris and D.L. Book - Flux-corrected Transport. III. Minimal-Error FCT Algorithms; *J.Comp.Phys.* 20, 397-431 (1976).

[11] G. Erlebacher - Solution Adaptive Triangular Meshes with Application to the Simulation of Plasma Equilibrium; *Ph.D. Thesis, Columbia University* (1984).

[12] A.K. Parrott and M.A. Christie - FCT Applied to the 2-D Finite Element Solution of Tracer Transport by Single Phase Flow in a Porous Medium; *Proceedings of the ICFD-Conf. on Numerical Methods in Fluid Dynamics*, Reading, Academic Press, 1986.

[13] R. Löhner, K. Morgan, M. Vahdati, J.P. Boris and D.L. Book - FEM-FCT: Combining High Resolution with Unstructured Grids; Submitted to *J.Comp.Phys.* (1986).

[14] K. Morgan, R. Löhner, J.R. Jones, J. Peraire and M. Vahdati - Finite Element FCT for the Euler and Navier-Stokes Equations; *Proc. 6th Int. Symp. Finite Element Methods in Flow Problems*, INRIA (1986).

[15] S.K. Godunov - *Mat. Sb.* 47, 271-306 (1959).

[16] J. Donea - A Taylor Galerkin Method for Convective Transport Problems: *Int.J.Num.Meth.Engng.* 20, 101-119 (1984).

[17] R. Löhner, K. Morgan and O.C. Zienkiewicz - The Solution of Nonlinear Systems of Hyperbolic Equations by the Finite Element Method; *Int.J.Num.Meth.Fluids* 4, 1043-1063 (1984).

[18] R. Löhner, K. Morgan and O.C. Zienkiewicz - An Adaptive Finite Element Procedure for High Speed Flows; *Comp.Meth.Appl.Mech.Eng.* 51, 441-465 (1985).

[19] R. Löhner, K. Morgan, J. Peraire and O.C. Zienkiewicz - Finite Element Methods for High Speed Flows; AIAA-85-1531-CP (1985).

[20] R. Löhner, K. Morgan, J. Peraire. O.C. Zienkiewicz and L. Kong - Finite Element Methods for Compressible Flow; pp. 28-53 in *Numerical Methods for Fluid Dynamics* (K.W. Morton and M.J. Baines eds.), Oxford University Press. (1986).

[21] M.A. Fry and D.L. Book - Adaptation of Flux-Corrected Transport Codes for Modelling Dusty Flows; *Proc. 14th Int.Symp. on Shock Tubes and Waves* (R.D. Archer and B.E. Milton eds.). New South Wales University Press (1983).

[22] D.E. Fyfe, J.H. Gardner, M. Picone and M.A. Fry - Fast Three-Dimensional Flux-Corrected Transport Code for Highly Resolved Compressible Flow Calculations; *Springer Lecture Notes in Physics* 218, 230-234, Springer Verlag (1985).

[23] G. Sod - *J.Comp.Phys.* 27, 1-31 (1978).

[24] A. Harten and Zwaas - Self-Adjusting Hybrid Schemes for Shock Computations; *J.Comp.Phys.* 6, 568-583 (1972).

[25] A.I. Zhmakin and A.A. Fursenko - A Class of Monotonic Shock-Capturing Difference Schemes; *NRL Memo. Rep.* 4567, (1981).

[26] R. Löhner - An Adaptive Finite Element Scheme for Transient Problems in CFD; to appear in *Comp.Meth.Appl.Mech.Eng.* (1987).

[27] J. Peraire, M. Vahdati, K. Morgan and O.C. Zienkiewicz - Adaptive Remeshing for Compressible Flow Computations; submitted to *J.Comp.Phys.* (1986).

[28] J.E. Carter - Numerical Solutions of the Navier-Stokes Equations for the Supersonic Laminar Flow Over a Two-Dimensional Compression Corner; *NASA Tech. Rep. R-385* (1972).

[29] H. Schlichting - *Boundary Layer Theory* ; Mc Graw Hill(1979).

[30] G. Patnaik, R.H. Guirguis, J.P. Boris and E.S. Oran - A Barely Implicit Correction for Flux-Corrected Transport; to appear in *J.Comp.Phys.* (1987).

[31] R. Löhner and K. Morgan - An Unstructured Multigrid Method for Elliptic Problems; to appear in *Int.J.Num.Meth.Eng.* (1987).

NELEM=1000 NPOIN=500
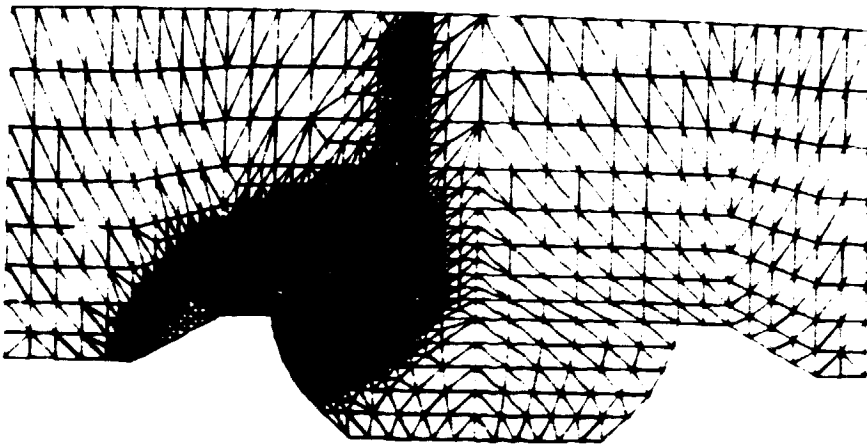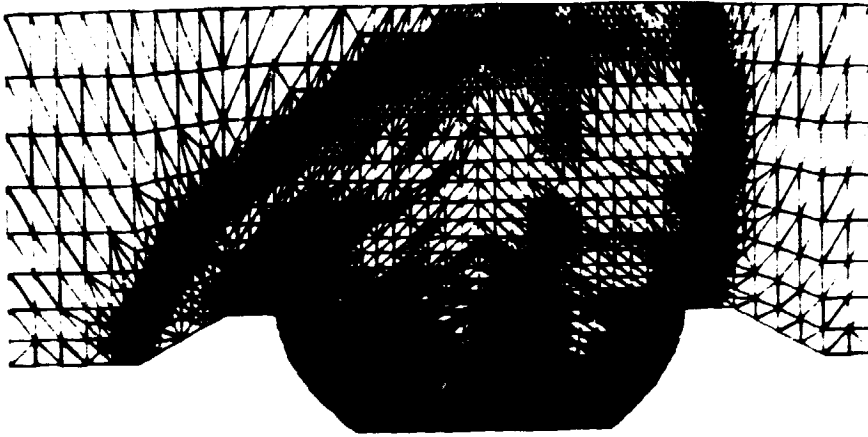
NELEM=11881, NPOIN=6073

DENSITY

NELEM=13433, NPOIN=6862
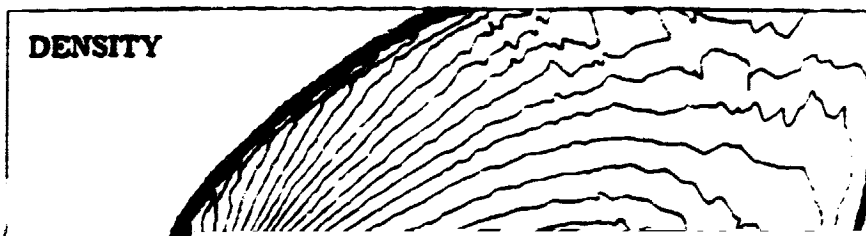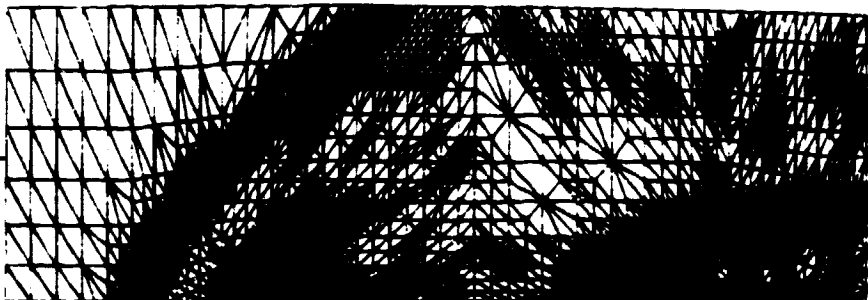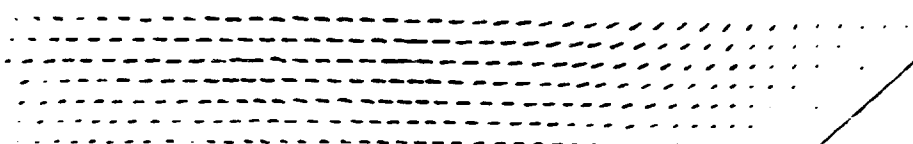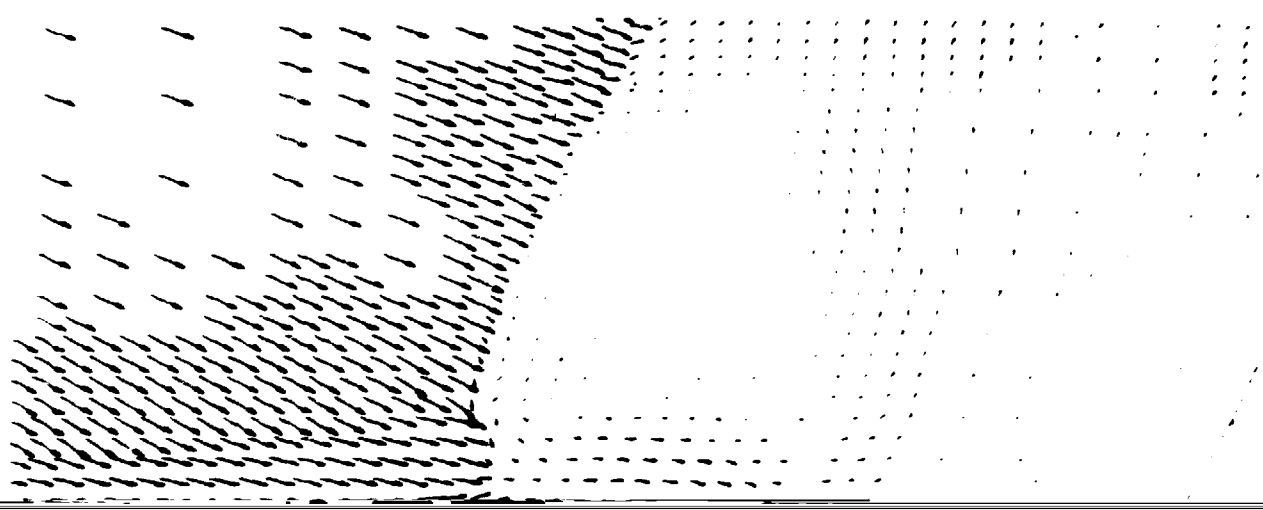
DENSITY

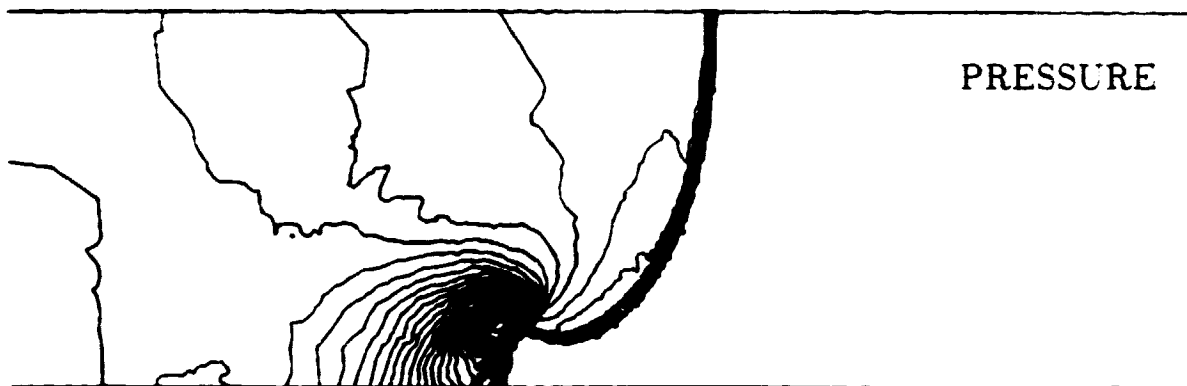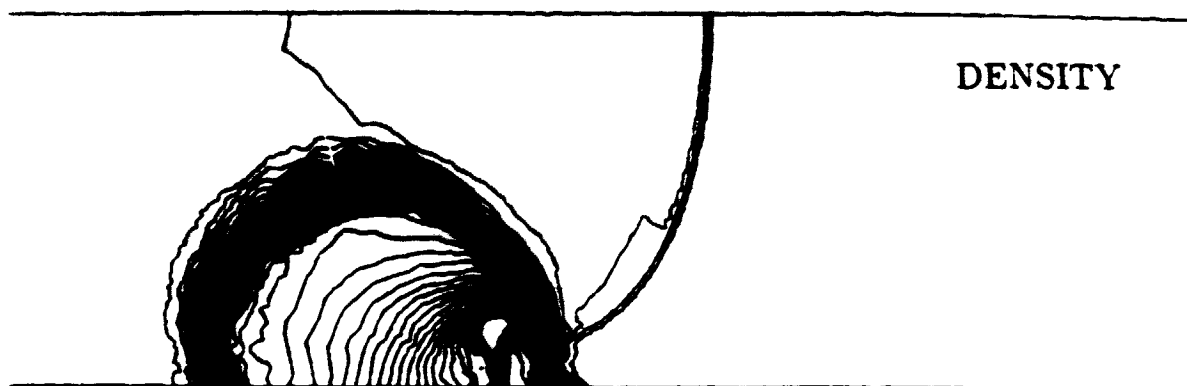T=0.12
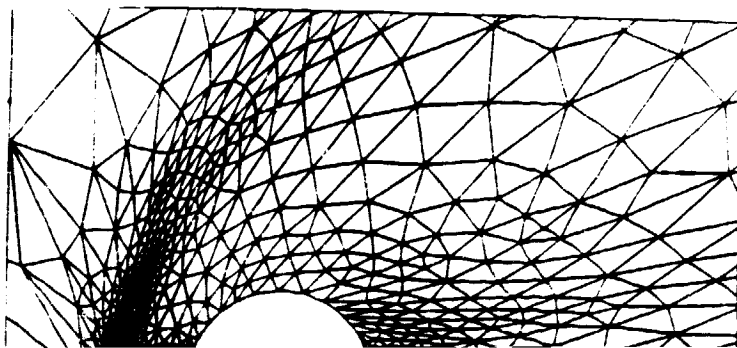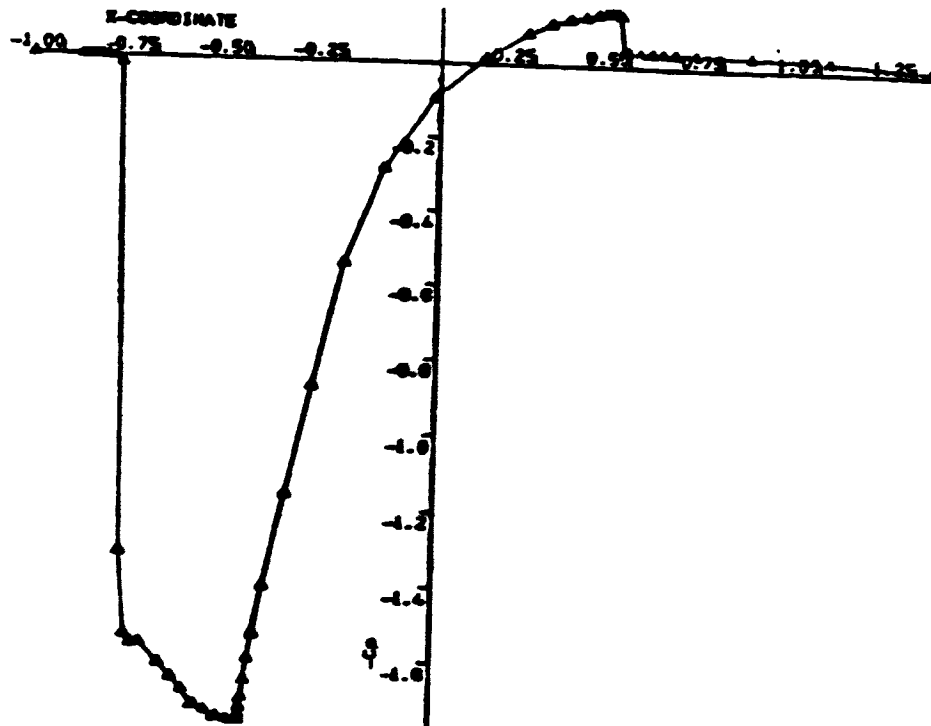
Figure 2: Steady supersonic flow past a cylinder

c) Variation of the pressure coefficient along the center line and over
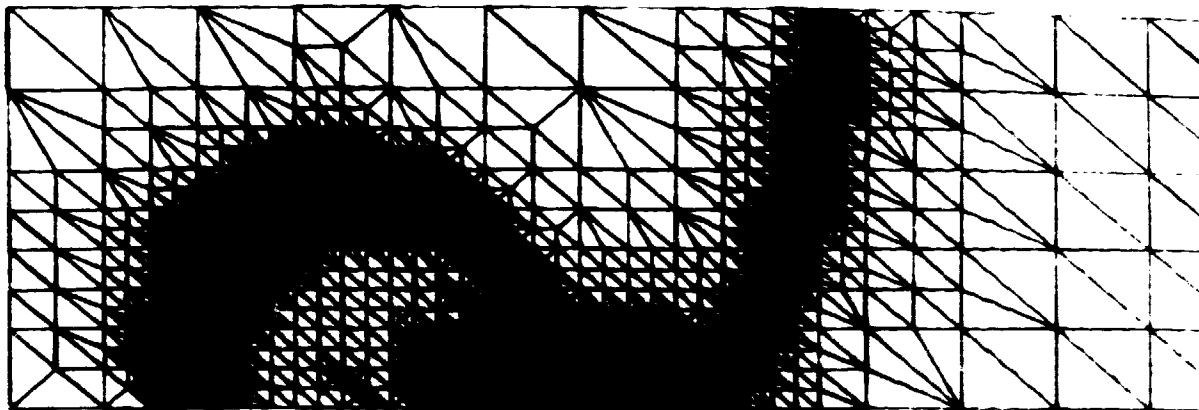the cylinder surface
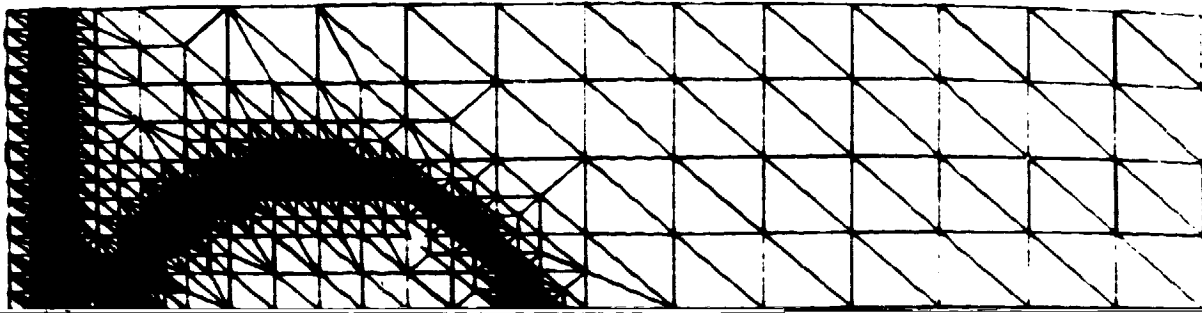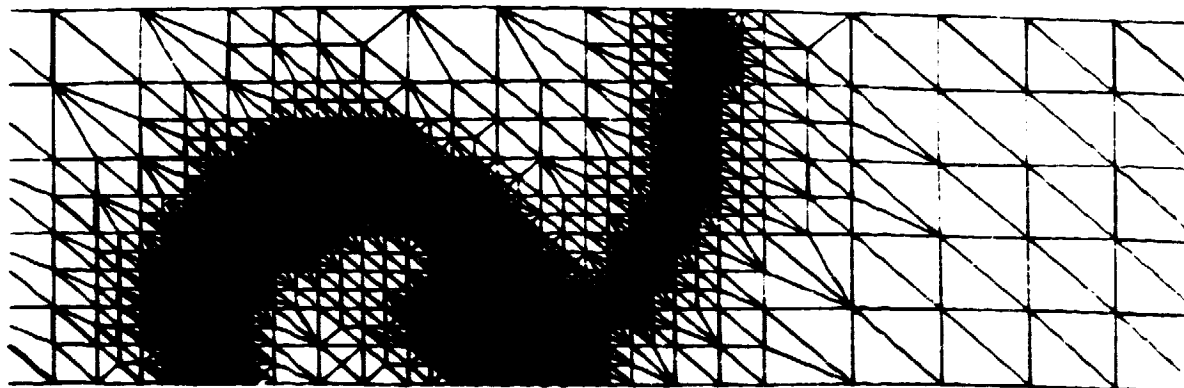
NELEM=14528, NPOIN=7335

DENSITY

PRESSURE

b)   T=0.6
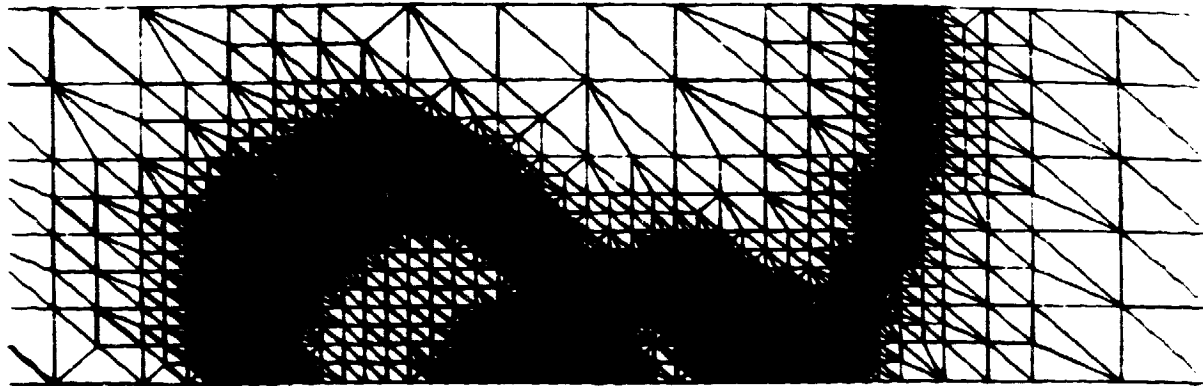
Figure 3: Shock-bubble interaction (cont.)

NELEM=16736, NPOIN=8464
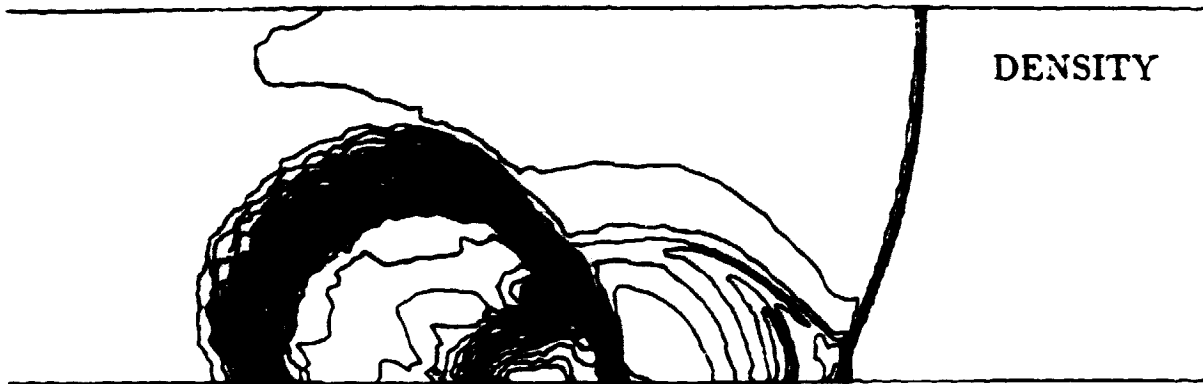

DENSITY
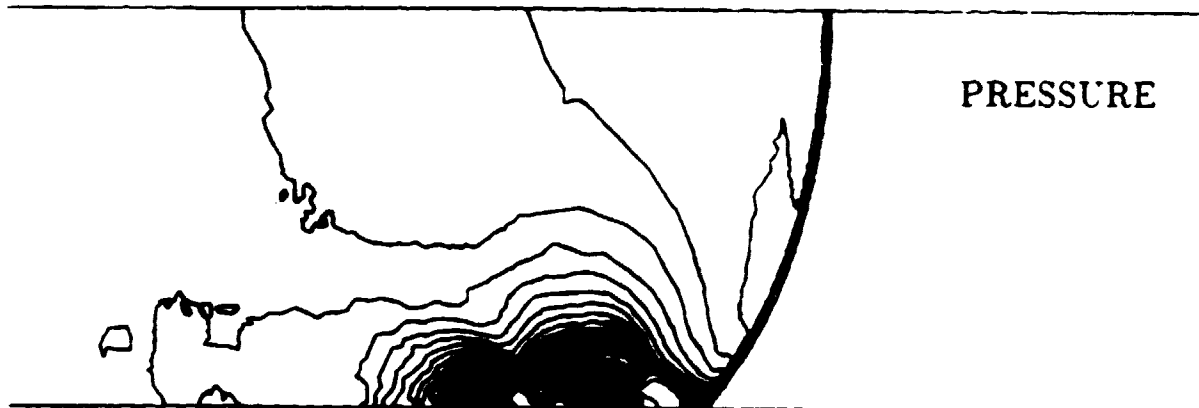
PRESSURE

c)

T=0.7

Figure 3: Shock-bubble interaction (cont.)

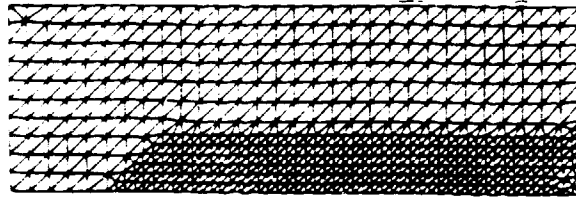NELEM=16577, NPOIN=8386

DENSITY

PRESSURE
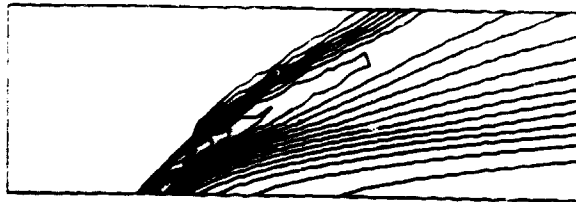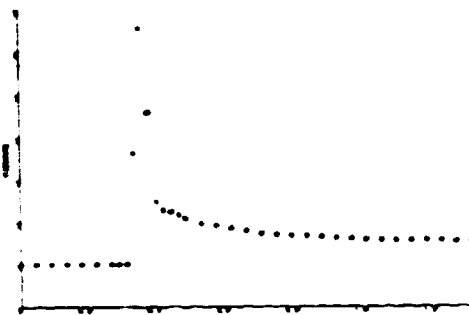
d)   T=0.8

Figure 3: Shock-bubble interaction (cont.)

(a)

(b)

(c)

FIGURE 4   MACH 3 FLOW PAST A FLAT PLATE REYNOLDS No. 1000
(a) Mesh,   (b) Density contours, (c) Pressure
variation along the line of the plate

23

Standard Bibliographic Page

1. Report No. NASA CR-178233 ICASE Report No. 87-4	2. Government Accession No.	3. Recipient's Catalog No.

4. Title and Subtitle	5. Report Date
FINITE ELEMENT FLUX-CORRECTED TRANSPORT (FEM-FCT) FOR THE EULER AND NAVIER-STOKES EQUATIONS	January 1987
	6. Performing Organization Code

7. Author(s)	8. Performing Organization Report No.
R. Lohner, K. Morgan, J. Peraire, M. Vahdati	87-4
	10. Work Unit No.

9. Performing Organization Name and Address Institute for Computer Applications in Science and Engineering Mail Stop 132C, NASA Langley Research Center Hampton, VA 23665-5225	11. Contract or Grant No. NAS1-17070, NAS1-18107
12. Sponsoring Agency Name and Address	13. Type of Report and Period Covered Contractor Report
National Aeronautics and Space Administration Washington, D.C. 20546	14. Sponsoring Agency Code 505-90-21-01

15. Supplementary Notes

Langley Technical Monitor: Submitted to Internat. J. Numer.
J. C. South   Methods Fluids

Final Report

16. Abstract

A high resolution finite element method for the solution of problems involving high speed compressible flows is presented. The method uses the concepts of flux-corrected transport and is presented in a form which is suitable for implementation on completely unstructured triangular or tetrahedral meshes. Transient and steady state examples are solved to illustrate the performance of the algorithm.

17. Key Words (Suggested by Authors(s))	18. Distribution Statement
compressible flow, finite element method, flux-corrected transport	34 - Fluid Mechanics and Heat Transfer 64 - Numerical Analysis Unclassified - unlimited

19. Security Classif.(of this report)	20. Security Classif.(of this page)	21. No. of Pages	22. Price
Unclassified	Unclassified	25	A02